J. Fluid Mech. (2005), *vol.* 541, *pp.* 193–202.
doi:10.1017/S0022112005006221 Printed in the United Kingdom

A time-dependent formulation of the mushy-zone free-boundary problem

By TIM P. SCHULZE[1] AND M. GRAE WORSTER[2]

[1]Department of Mathematics, University of Tennessee, Knoxville, TN 37996-1300, USA

[2]Institute of Theoretical Geophysics, Department of Applied Mathematics and Theoretical Physics, Centre for Mathematical Sciences, Wilberforce Road, Cambridge CB3 0WA, UK

(Received 9 March 2005 and in revised form 1 July 2005)

We present time-dependent governing equations and boundary conditions for the mushy-zone free-boundary problem that are valid in an arbitrary frame of reference. The model for time-evolving mushy zones is more complicated than in the steady case because the interface velocity $\boldsymbol{w}$ can be distinct from both the velocity of the dendrites $\boldsymbol{v}$ and the fluid velocity $\boldsymbol{u}$. We consider the limit of negligible solutal diffusivity, where there are four types of boundary condition at the mush–liquid interface, depending on both the direction of flow across the interface and the direction of the interface motion relative to the solid phase. We illustrate these boundary conditions by examining a family of one-dimensional problems in which a binary material is chilled from a fixed cold point in the laboratory frame of reference while fluid is pumped through the resulting mushy layer at a rate Q and the mushy layer itself is translated at a rate V. This allows us to exhibit three of the four types of mushy-layer interfaces. We show that the fourth type cannot occur in this scenario.

1. Introduction

Mushy zones are porous layers of dendritic crystals that commonly form during solidification of multi-component melts. Much of the research on this topic has focused on binary mushy zones modelled as a homogenised liquid–solid phase (see Worster 1997 for a review specific to mushy zones and Davis 2001 for a more general survey of solidification).

While it is possible for portions of the mushy zone to break free and move relative to one another, in most situations the solid phase of the mushy layer forms a single rigid structure that changes only by solidification or melting. In this case it is often natural to adopt a frame of reference in which the solid is stationary. Indeed, most, if not all, models for mushy zones have this assumption built into them in such a way that the equations fail to be Galilean invariant. Since many manufacturing processes feature continuous solidification at a constant rate, it is also common to adopt a frame of reference in which the solid moves at a uniform velocity. Owing to the lack of Galilean invariance, this change of coordinates modifies the governing equations and leaves one with a model in which velocities and positions are measured in separate frames of reference. While this is a common practice in the solidification literature, it can lead to confusion and inconvenience in analysing general situations where the interface and the solid-phase velocity are distinct.

We present the mushy-layer free-boundary problem for time-dependent flows in the limit of negligible solutal diffusivity. This limit is relevant to real systems as the ratio

of thermal to solutal diffusivity is normally very large. An alternative, not described here, would be to attempt to resolve the thin solutal boundary layers that form near interfaces where fluid flows into mushy zones, but this can be problematic from a computational point of view because of the need to resolve the boundary layer. Beckermann & Wang (1995) give a review focusing on more comprehensive models of this type, especially those adopting a single-domain, smeared-interface model. An important consideration in choosing between the single-domain and sharp-interface models is that the liquidus constraint applied within the mushy layer essentially slaves the solute field to the thermal field, so that the character of the solute-evolution equation changes from parabolic for concentration to hyperbolic for solid fraction. The complication in the present case, which was identified by Schulze & Worster (1999) and is discussed further in Worster (2002) for steady scenarios, is that the thermodynamic boundary conditions at the mush–liquid interface come in four distinct types, depending on the direction of flow across the interface and whether the interface is freezing or dissolving. Below, we describe in detail how to extend these results to the time-dependent scenario.

In the next section we briefly present a mushy-layer model valid in arbitrary frames of reference and address the issue of boundary conditions for this time-dependent formulation of the sharp-interface model. We then illustrate some of the subtleties that can emerge by examining various solidification regimes that can be brought about by combinations of solidification and fluid velocities in a one-dimensional solidification geometry.

2. Governing equations

Mushy-layer models are built around two central assumptions. First, one assumes the system can be treated using local averages over regions that are small compared to the size of the system being investigated, yet span enough of the microstructure to be representative. Within the mushy layer, all of the variables are assumed to be averaged in some way. In some cases this average is over regions containing just one of the two phases and in other cases the average is a volume-fraction weighted average over the liquid and solid portions of a local region. Since we shall assume equal densities in all phases, we make no distinction between mass and volume. The second assumption is that the solid fraction adjusts to maintain a local equilibrium where the interstitial (i.e. liquid) concentration is always equal to the liquidus concentration.

The model for time-evolving mushy zones is more complicated than in the steady case because the interface velocity $\boldsymbol{w}$ can be distinct from both the velocity of the dendrites $\boldsymbol{v}$ and the fluid velocity $\boldsymbol{u}$. The solid velocity will be spatially uniform and, as a result, requires no averaging and is simply equal to the velocity of a point embedded in the dendrites. The fluid velocity is an average over the fluid portion of a representative region. Note that the interface is not a material interface, but rather a moving boundary that marks, in an averaged sense, the envelope that bounds the region containing dendrites. When this region is expanding relative to material points embedded in the dendrites, we shall say the interface is a freezing interface; when it is shrinking we shall say the interface is a dissolving interface. This is distinct from internal phase change where the solid fraction may be increasing or decreasing at a point within the interior of the mushy region irrespective of the boundary's motion. While these three velocities are sufficient to formulate the model, one often finds that other combinations are convenient. In particular, we favour the total flux vector $\boldsymbol{q} = \chi \boldsymbol{u} + \phi \boldsymbol{v}$, where ϕ and $\chi = 1 - \phi$ are the local solid and liquid volume fractions

in the mushy zone, in place of the fluid velocity, as it has the advantage of being divergence free and its normal component is continuous at all interfaces. Two other quantities that can be useful are the flux of liquid $\chi \boldsymbol{u}$ and, more commonly, the Darcy flux $\chi(\boldsymbol{u}-\boldsymbol{v}) = \boldsymbol{q}-\boldsymbol{v}$, which is the flux of liquid relative to the solid phase. Below, we indicate Lagrangian derivatives moving with the velocities $\boldsymbol{v}$, $\boldsymbol{u}$ and $\boldsymbol{q}$ using an s, l and no superscript, respectively.

For brevity, we restrict our attention to the bulk equations in the mushy zone. These equations represent conservation of mass, solute and heat, supplemented here by Darcy's law for momentum transport:

$$\nabla\cdot\boldsymbol{q} = 0, \tag{2.1}$$

$$\frac{\mathrm{D}C}{\mathrm{D}t} - \phi\frac{\mathrm{D}^s C}{\mathrm{D}t} = (C-C_s)\frac{\mathrm{D}^s\phi}{\mathrm{D}t}, \tag{2.2}$$

$$\frac{\mathrm{D}T}{\mathrm{D}t} = \kappa\nabla^2 T + \mathscr{L}\frac{\mathrm{D}^s\phi}{\mathrm{D}t}, \tag{2.3}$$

$$\boldsymbol{q}-\boldsymbol{v} = -\frac{\Pi(\phi)}{\mu}(\nabla p - \rho\boldsymbol{g}). \tag{2.4}$$

It can be readily confirmed that these equations reduce to those describing an ideal mushy layer (Worster 1997) in the case $\boldsymbol{v} = 0$. The parameters are the diffusivity κ, viscosity μ, concentration in the solid phase C_s, the latent heat per unit volume $\mathscr{L}$ and a permeability $\Pi(\phi)$ that is a function of the local solid fraction. Since all time derivatives are expressed in Lagrangian form, these equations are valid in any inertial frame of reference and, with the exception of Darcy's law (2.4), also apply in the liquid region with $\boldsymbol{v} = \phi = 0$. Within the mushy zone, this system of equations is closed by the liquidus constraint $T = T_L(C)$. In § 3, we shall use the linear model

$$T = T_E + \Gamma(C - C_E), \tag{2.5}$$

where T_E and C_E are the eutectic temperature and concentration. We shall operate on the side of the phase diagram with $C < C_s$, so that $\Gamma > 0$, and take $C_s = 1$.

The standard boundary conditions applied at an interface between a liquid and a porous medium are continuity of normal mass flux and continuity of pressure, along with either a condition of no slip relative to the solid phase or a slip condition between the Darcy flux and the fluid velocity, measured relative to the solid phase, on the liquid side of the interface (Beavers & Joseph 1967). It is feasible, however, that the appropriate condition at mush–liquid interfaces is continuity of all components of the liquid velocity in cases where the solid fraction approaches zero at the interface. In particular, we shall see below that this latter condition is consistent with a solid-fraction profile that has a vanishing derivative moving with the solid phase at the interface when liquid and solid have equal thermal properties. For the special case of flows which are normal to the boundary, like the examples considered in § 3, the issue of slip between fluid velocity and Darcy flux does not arise.

The temperature is governed by the same second-order PDE in both regions and requires two jump conditions at the mush–liquid interface, namely

$$[T]_l^m = 0, \tag{2.6}$$

$$\kappa[\hat{\boldsymbol{n}}\cdot\nabla T]_l^m = \mathscr{L}(\boldsymbol{w}-\boldsymbol{v})\cdot\hat{\boldsymbol{n}}\,\phi, \tag{2.7}$$

where $\hat{\boldsymbol{n}}$ is the mush-to-liquid normal, and the square brackets with l and m sub/superscripts indicate the jump in the enclosed quantity across the interface. The first of these follows from imposing continuity of temperature and the other

	Inflow $(\boldsymbol{q}-\boldsymbol{w})\cdot\hat{\boldsymbol{n}}<0$	Outflow $(\boldsymbol{q}-\boldsymbol{w})\cdot\hat{\boldsymbol{n}}>0$
Freezing $(\boldsymbol{v}-\boldsymbol{w})\cdot\hat{\boldsymbol{n}}<0$	A: $T = T_L(C_{\mathrm{in}})$	C: $\dfrac{\mathrm{D}T}{\mathrm{D}t}=0$
Dissolving $(\boldsymbol{v}-\boldsymbol{w})\cdot\hat{\boldsymbol{n}}>0$	B: $[C]_l^m(\boldsymbol{q}-\boldsymbol{w})\cdot\hat{\boldsymbol{n}} = \phi(C\|^m - C_s)(\boldsymbol{v}-\boldsymbol{w})\cdot\hat{\boldsymbol{n}}$	D: $\phi = 0$

TABLE 1. The boundary condition that determines the interface position for the four interface types described in the text.

by integrating the conservation equation (2.3) across the boundary. When this is done, terms that are singular make a contribution to the boundary condition. These singularities, in turn, arise from derivatives of discontinuous quantities, which may include both the temperature gradient and the solid fraction at the interface. Thus the divergence of the temperature gradient, the gradient of the solid fraction and the time derivative of the solid fraction can be singular. Note that we can avoid the third singularity by considering a frame of reference that moves with the instantaneous interface velocity, so that the time derivative of the solid fraction will be spatially discontinuous, but non-singular. Writing the remaining singular terms in divergence form and applying the divergence theorem then gives the appropriate boundary condition in terms of the solid-phase velocity in this particular frame of reference. To restore Galilean invariance, we express the result in terms of the solid-phase velocity relative to the interface position.

While the boundary conditions for the thermal and velocity fields are derived from elliptic PDEs, those relating to the solute field and solid fraction are derived from hyperbolic equations. In the liquid, the solute field is governed by an ODE along characteristics which follow the streamlines, while in the mushy region the solid fraction is governed by an ODE along characteristics that follow the solid phase. The type of interface condition one needs to apply depends upon which way these characteristics intersect the interface. There are four possibilities, which we discuss in turn and summarize in table 1.

In the absence of solute diffusion, continuity of concentration can only be enforced in the case that the fluid flows from the mush to the liquid region. Thus

$$[C]_l^m = 0 \quad \text{when} \quad (\boldsymbol{q}-\boldsymbol{w})\cdot\hat{\boldsymbol{n}} > 0. \tag{2.8}$$

Note that it is the normal component of the fluid velocity on the liquid side of the interface, which is equal to the normal component of the mass flux $\boldsymbol{q}\cdot\hat{\boldsymbol{n}}$, that matters. While the latter is continuous, the normal component of the fluid velocity is discontinuous whenever the solid fraction is. The fluid can even change direction relative to the interface if the solid phase is moving sufficiently fast in the same direction as the fluid on the liquid side of the interface. The same cautions apply to the fluid flux $\chi\boldsymbol{u}$. Within the mushy regions, there is no need for solute boundary conditions, as concentration is determined by the liquidus constraint (2.5). As will be seen shortly, however, conservation of solute plays a role either in determining the solid fraction along freezing interfaces or in determining the location of the free boundary along dissolving interfaces.

With the concentration determined by the liquidus constraint, (2.2) serves as a first-order hyperbolic PDE for the solid fraction. The characteristic curves are determined by the velocity of the solid phase and, as a result, boundary conditions are needed along freezing interfaces, characterized by $(\boldsymbol{v}-\boldsymbol{w})\cdot\hat{\boldsymbol{n}}<0$. The appropriate condition follows from integrating (2.2) in a region that collapses onto the interface. Because the solutal diffusivity is taken to be zero, C can be discontinuous and terms involving its first derivative give a contribution to the fluxes at the interface. Writing (2.2) in conservation form, we obtain

$$[(1-\phi)(C-C_s)]_t+\nabla\cdot[C\boldsymbol{q}+(C_s-C)\phi\boldsymbol{v}]=0,$$

and following the procedures used in deriving (2.7) we find

$$[C]_l^m(\boldsymbol{q}-\boldsymbol{w})\cdot\hat{\boldsymbol{n}}=\phi(C|^m-C_s)(\boldsymbol{v}-\boldsymbol{w})\cdot\hat{\boldsymbol{n}}. \tag{2.9}$$

Note that when flow is into the liquid region, continuity of concentration (2.8) combines with this jump condition to imply $\phi=0$ on the interface (box D in table 1); when flow is in the other direction, however, there can be a finite jump in solid fraction and (2.9) must be used in full (box B in table 1).

The location of a mush–liquid interface is determined solely by (2.9) along dissolving interfaces but additionally by a principle of marginal equilibrium along freezing interfaces (Worster 1986; Schulze & Worster 1999). The idea behind the principle of marginal equilibrium is that the mushy zone grows so as to prevent supercooled regions from forming. When flow is into the mushy zone, one can extend the liquidus constraint to the liquid side of the interface, which will then combine with continuity of temperature to give continuity in concentration. As a consequence, the interface is pinned at precisely the point where the temperature meets the liquidus *from above* as fluid moves toward the mushy region (box A in table 1).

When the flow is from the mush to the liquid region, the situation is more subtle. By continuity, the temperature is equal to its liquidus value at the interface and, given that C is constant moving with the liquid, we must have $\mathrm{D}T/\mathrm{D}t|^l\geqslant 0$, so that the temperature locally rises as one moves with the flow on the liquid side of the interface. This is the original, one-sided marginal equilibrium of Worster (1986). Since $\phi=0$, owing to conservation of solute and continuity of C, both the temperature and its gradient are continuous. If we further assume that the fluid velocity is continuous, we can extend this inequality to the mush side of the interface. This additional assumption can be relaxed in a unidirectional situation like the examples we consider in § 3. In any event, a smooth velocity field combines with the liquidus relationship (2.5) to give $\mathrm{D}C/\mathrm{D}t|^m\geqslant 0$.

Since the interface is freezing and the solid fraction is zero on the interface, the solid fraction cannot decrease as we follow the solid phase, implying that $\mathrm{D}^s\phi/\mathrm{D}t|^m\geqslant 0$. This condition can be combined with (2.2) to give the opposite of the previous inequality for the Lagrangian derivative of the concentration, namely $\mathrm{D}C/\mathrm{D}t\big|^m\leqslant 0$, which then implies

$$\left.\frac{\mathrm{D}C}{\mathrm{D}t}\right|^m=\left.\frac{\mathrm{D}^s\phi}{\mathrm{D}t}\right|^m=\frac{\mathrm{D}T}{\mathrm{D}t}=0\quad\text{on the interface} \tag{2.10}$$

(box C in table 1). This is the time-dependent generalization of the boundary condition derived by Schulze & Worster (1999) for determining the location of mush–liquid interfaces in cases where flow passes out of the mushy zone along a freezing boundary. The condition implies that the rate of change of the temperature field with time moving with velocity $\boldsymbol{q}$ is zero at the interface.

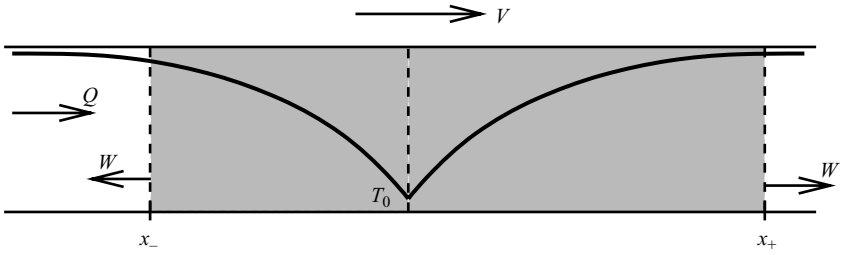

FIGURE 1. A diagram of the solidification experiment analyzed in the text, including a sketch of the imposed temperature profile.

3. Examples

To illustrate some of the situations that can be encountered, we consider solidification with an imposed, uniform flow $\boldsymbol{q} = Q\boldsymbol{i}$ in a unidirectional geometry (figure 1). In principle, such a flow could be established by confining the solidifying material to a Hele-Shaw cell. Note that while the mass flux is constant at any instant, the liquid velocity varies within the mushy region. In addition to this constant flow rate, one can require the cell (and the solid phase attached to it) to translate parallel to the flow with velocity $\boldsymbol{v} = V\boldsymbol{i}$. These pumping and pulling velocities are relative to a laboratory frame of reference in which a time-dependent temperature profile is imposed. The novelty here, with respect to the conventional 'directional solidification' scenario, is that the 'pulling velocity' V and the flow velocity Q can be imposed independently of one another, whereas they are normally the same. For solidification without a mushy zone or for solidification below the eutectic temperature, this would be impossible because the solid would be impermeable. Thus it is important to impose a temperature $T_L(C_{\mathrm{in}}) > T_0 > T_E$ that is between the liquidus temperature of the far-field concentration C_{in} and the eutectic temperature, so that no completely solid regions form.

To perform such an experiment most easily, one would constrain the temperature at a fixed point $x = 0$ in the laboratory frame of reference and move solidifying fluid past this point while thermally insulating the remainder of the cell. Modelling this situation requires fully coupled thermal and mass transport, but we shall simplify our illustration by assuming that the temperature is imposed externally along the entire length of the domain. While not especially realistic, this approximates a situation where the Hele-Shaw cell has good thermal contact with a high-heat-capacity medium, so that the temperature is communicated through the walls of the cell at a rate that is fast compared to any heat transport occurring along the cell. If we combine this assumption with one of negligible latent heat, we can decouple the thermal and flow fields and allow a convenient similarity solution for the heat equation on two adjacent, semi-infinite, one-dimensional subdomains with the initial condition $T(x, 0) = 0 > T_L(C_{\mathrm{in}})$ for $x \neq 0$ and an imposed constant temperature $T(0, t) = T_0$ at the common point $x = 0$ of the two subdomains. In this case

$$T(x, t) = T_0[1 - \mathrm{erf}(|\eta|/2)], \tag{3.1}$$

where κ is the thermal diffusivity, $\eta = x/\sqrt{\kappa t}$ is the similarity variable and the error function is defined as

$$\mathrm{erf}(z) = \frac{2}{\sqrt{\pi}} \int_0^z \mathrm{e}^{-s^2}\, \mathrm{d}s.$$

Notice that this imposed temperature profile has a discontinuous derivative at $x = 0$. This will be reflected in the concentration within the mushy zone through the local equilibrium condition and in the solid fraction, which adjusts to maintain local equilibrium. As a result, there will be discontinuities in the derivative of the solid fraction profile at the head $x = 0$ and tail $x = Vt$ of the solid-fraction characteristic that emerges from the origin since characteristics that lie entirely outside of this region do not require integrating over the discontinuity in the concentration field.

Within the mush, the concentration $C(x, t)$ is determined by the temperature through the liquidus constraint, while in the liquid it is determined by either the initial or effluent concentrations:

$$C(x,t) = \begin{cases} C_{\text{in}} & \text{if upstream or far-stream} \\ C_E + \Gamma^{-1}(T - T_E) & \text{in mushy zone} \\ C_{\text{out}} & \text{if downstream.} \end{cases} \tag{3.2}$$

Note that to be 'downstream', a point must be in the liquid, the flow must be out of the mushy layer and there must have been time for the effluent to reach the point in question. It is possible for both the forward and backward moving fronts to be upstream, but only one can be downstream. We will not explicitly determine the concentration of the effluent except to note whether it is lower or higher than the initial value C_{in}, as it is not needed to determine interface locations nor the solid fraction profile.

The solute conservation equation (2.2) reduces to a one-dimensional, first-order PDE for the solid fraction

$$\phi_t + V\phi_x = \left(\frac{C_t + VC_x}{1 - C}\right)\phi + \frac{C_t + QC_x}{C - 1}, \quad x_- < x < x_+, \tag{3.3}$$

where the mushy-layer domain (x_-, x_+) is to be determined as part of the solution. Thus, despite its simple one-dimensional structure, this free-boundary problem exhibits many of the essential difficulties associated with the full model. If we move to the frame of reference moving with the dendrites, so that $\xi = x - Vt$, this becomes a first-order ODE for the solid fraction $\phi(t;\xi)$, parameterized by the moving coordinate ξ:

$$\phi_t - \frac{C_t}{1 - C}\phi = \frac{C_t + (Q - V)C_\xi}{C - 1}, \quad x_- - Vt < \xi < x_+ - Vt. \tag{3.4}$$

The solution to (3.4) is

$$\phi(t;\xi) = \frac{C(t_0;\xi) - C(t;\xi)}{1 - C(t;\xi)} - \frac{Q - V}{1 - C(t;\xi)} \int_{t_0(\xi)}^{t} C_\xi \, \mathrm{d}t, \tag{3.5}$$

where the integration of the function $C_\xi(t;\xi)$ along the characteristics must begin at the time that solidification was initiated $t_0(\xi)$, which is determined by the solution to the free-boundary problem.

To determine the free-boundary locations we must consider specific cases. We present two examples here; both have $\Gamma = \kappa = 1$, $\mathscr{L} = 0$, $T_E = -1$, $C_E = 0.5$, $C_{\text{in}} = 0.75$ and $T_0 = -0.9$. First we consider a case where $V > Q > 0$ ($V = 0.14$ and $Q = 0.115$). In figure 2(*a*)(i), we show the location of the interface in a space–time plot along with the characteristic curves for solid fraction and solute concentration. In figure 2(*a*)(ii), we graph the solid fraction at three times. The isotherms are moving at a rate proportional to $t^{-1/2}$, so that they slow down with time. For $x > 0$ and early times, we will have $W > V > Q > 0$ and, for $x < 0$ we will have $V > Q > 0 > W$, so that the net

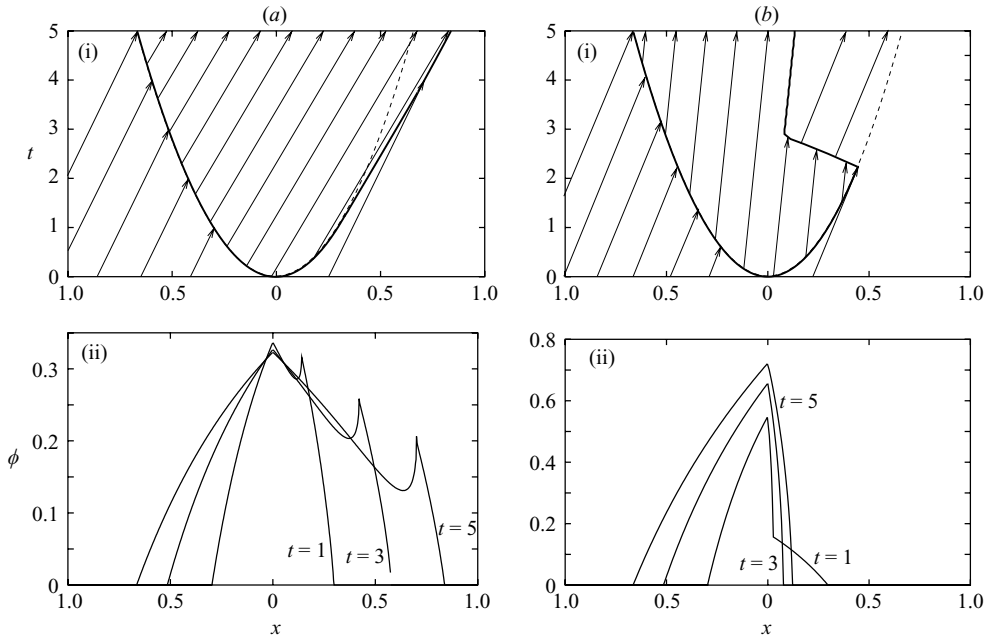

FIGURE 2. (*a*)(i) A space–time diagram showing the interface position (solid curve), the isotherm $\eta = \eta_1$ (dashed where it fails to coincide with the interface), solid-fraction characteristics in the mushy zone (solid with arrows) and concentration characteristics in the liquid (solid with arrows) for the case with $V > Q > 0$. (*a*)(ii) A corresponding graph of the solid fraction at three times, where the location of the rightward moving interface is governed by the conditions $T = T_L(C_{\rm in})$, equation (2.9) and $\phi = 0$. Note that the solid fraction is discontinuous at $t = 3$. These three cases also correspond to figure 3(*a*), 3(*c*) and 3(*d*). (*b*)(i) Analogous to (*a*)(i) for the case $Q > V > 0$. (*b*)(ii) Corresponding graph of the solid fraction at three times, where the location of the rightward moving interface is governed by the conditions $T = T_L(C_{\rm in})$ and $\phi = 0$. Note that the interface changes direction twice. These two cases correspond to figures 3(*a*) and 3(*b*).

flow is into the mushy layer along a freezing interface on both ends of the domain (box A of table 1). This remains the case, for both examples, at $x = x_{-}(t)$, so that all transitions will be on the right half of the domain. For this type of boundary, the far-field concentration is communicated to the interface, which is then pinned at the freezing point dictated by the phase diagram (see figure 3*a* and discussion below). Thus, the free boundaries simply follow the parabolic isotherm $T = T_L(C_{\rm in})$, which corresponds to a constant values of $\eta = \pm\eta_1$, where $\eta_1 > 0$ satisfies

$$T_0[1 - \mathrm{erf}(\eta_1/2)] = T_E + \Gamma(C_{\rm in} - C_E).$$

The velocity of this first type of interface is then $W_1 = \eta_1\sqrt{\kappa/t}\,\mathrm{sgn}(x)/2$. Also, the time $t_0(\xi)$ that solidification began along characteristic ξ is determined by the intersection of the characteristic with the isotherm at time $t_0 = (\kappa\eta_1^2 - 2\xi V - \sqrt{D})/(2V^2)$, where the discriminant $D = \kappa^2\eta_1^4 - 4\xi V\kappa\eta_1^2$ must be non-negative for there to be an intersection. When $D = 0$ the characteristic is tangent to the isotherm in the space–time plot and, in the limit $V \to 0$, we have $t_0 \to (\xi^2)/(\eta_1^2\kappa)$.

A very useful perspective on the behaviour of mushy zones is gained by examining where the local state of the system falls on the equililbrium phase diagram as we move around the physical domain. In figure 3, we present several versions of the solute-rich

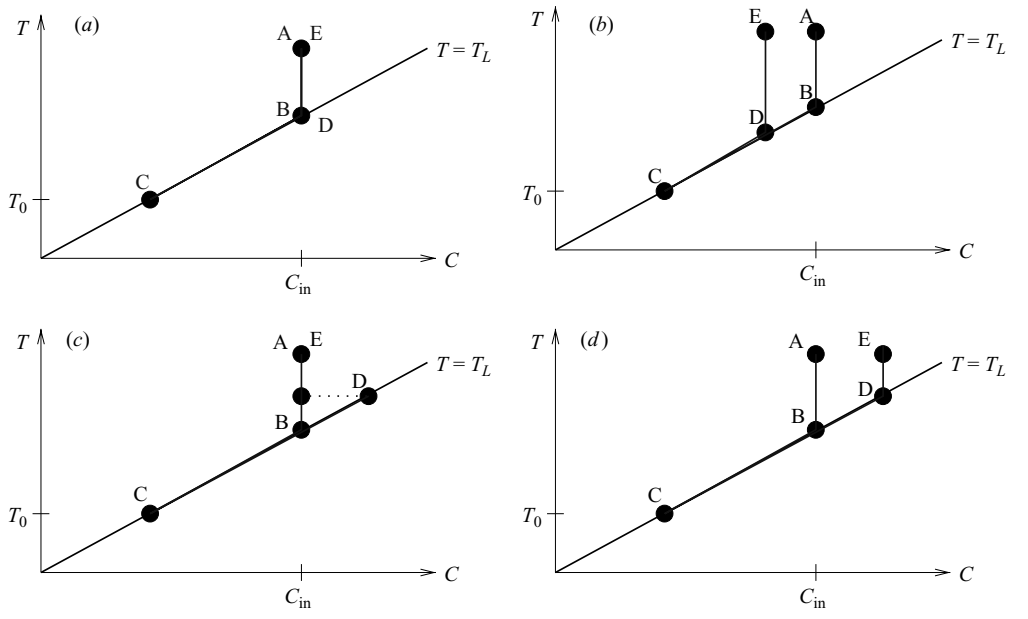

FIGURE 3. Portions of four phase diagrams, showing a linear liquidus curve along with paths denoting the state of the system at the far left (A), the left interface (B), $x = 0$ (C), the right interface (D) and the far right (E). The four diagrams correspond to the state of the system at times (*a*) $t = 1$, (*b*) $t = 3$ and (*c*) $t = 5$ in figure 2(*a*) and (*a*) $t = 1$ and $t = 3$ and (*b*) $t = 5$ in figure 2(*b*).

side of a diagram with a linear liquidus and vertical solidus, which are the conditions we assume govern the behaviour of our examples. On these diagrams we have drawn several paths, with points labelled A to E, that mark out the state of the system as one sweeps from left to right at the same instant of time under various operating conditions. The first diagram, for example, indicates the scenario just described, where material is entering the mushy zone on both the left and right side of the interface at a temperature that is dictated by the inlet concentration C_{in}. Note that when material is in the liquid region, its concentration is fixed along these paths, and when it is in the mushy zone, the concentration is dictated by the local temperature. It is also possible for material to cross one of the interfaces at a concentration above or below this value or to have a discontinuous concentration at the interface, depending on parameter choices and the time the diagram is drawn. The remaining three cases are discussed below in the contexts provided by figure 2.

As the interfaces slow down in our first example, the situation on the right changes when the pulling velocity V first exceeds W. This occurs at a time $t_V = \kappa(\eta_1/V)^2/4$ and a position $x_V = \eta_1^2\kappa/(2V)$. The boundary is then a dissolving interface with flow into the mushy layer (box B of table 1). As the pre-existing mushy layer is forced through the boundary, some of it dissolves to reconcile its concentration with the inlet concentration C_{in}. The result is a discontinuity in the solid fraction at the right side of the domain, as illustrated in figure 2(*a*)(ii) at time $t = 3$. This situation persists until the rightward-moving interface, which now moves faster than the isotherm $\eta = \eta_1$, slows to the point where $W = Q$, when the interface changes pace once again to satisfy the boundary condition $\phi = 0$ (box D of table 1). In this latter situation the

flow is out of the mushy layer so that solute leaves with a concentration fixed at values that are higher than the initial concentration C_{in} (see figure 3*d*).

For our second example, we consider the case $Q > V > 0$ (figure 2*b*), with $V = 0.025$ and $Q = 0.1$. At early times, the situation is analogous to our first example, but at time $t_Q = \kappa(\eta_1/Q)^2/4$ and a position $x_Q = \eta_1^2$, the interface has slowed so that the flow is out of the mushy layer. If the rightward-moving interface were to remain a freezing interface with $W > V$, this would be the fourth and final boundary type (box C of table 1), but it turns out this cannot occur for any choices of V and Q. This can be seen by realizing that the boundary condition (2.10), rewritten as $-T_t/T_x = Q$, prescribes the velocity of the isotherm that the interface is instantaneously attached to. Using (3.1), however, we calculate $W_2 = -T_t/T_x = 2Q$, which would indicate that any potential fronts of this type move faster than the flow – a contradiction. Instead, the interface begins to retreat, so that $V > W$, and the condition $\phi = 0$ is once again the appropriate choice. Unlike the first example, however, the effluent concentration is now lower than the initial value C_{in} (figure 3*b*). Note that the retreat of the interface is eventually halted when it attaches itself to the characteristic emerging from $x = 0$.

4. Conclusion

In this paper, we have presented a time-dependent model for the evolution of a mushy zone valid in arbitrary frames of reference and described boundary conditions that apply in various scenarios. As the examples in § 3 show, it is possible for interfaces to make transitions between these interface types and one must take care to identify the correct condition to apply. While the effect of implementing the boundary conditions incorrectly may not be readily apparent – indeed may even lead to a 'smoother' solution – doing so can lead to solutions that do not conserve the mass of each species present. The effects are subtle and will probably prove difficult to implement in a robust manner for large calculations that are meant to adapt to arbitrary topology changes and changes in boundary type. In particular, the need to distinguish between interface types does not go away if one adopts a single-domain model owing to the underlying hyperbolic nature of (2.2) when viewed as an evolution equation for the solid fraction.

The authors would like to acknowledge support from the National Science Foundation through grant number DMS–0405650.

REFERENCES

Beavers, G. S. & Joseph, D. D. 1967 Boundary conditions at a naturally permeable wall. *J. Fluid Mech.* **30**, 197–207.

Beckermann, C. & Wang, C. Y. 1995 Multiphase/scale modeling of alloy solidification. *Annu. Rev. Heat Transfer* **6**, 115–198.

Davis, S. H. 2001 *Theory of Solidification.* Cambridge University Press.

Schulze, T. P. & Worster, M. G. 1999 Weak convection, liquid inclusions and the formation of chimneys in mushy layers. *J. Fluid Mech.* **388**, 197–215.

Worster, M. G. 1986 Solidification of an alloy from a cooled boundary. *J. Fluid Mech.* **167**, 481–501.

Worster, M. G. 1997 Convection in mushy layers. *Annu. Rev. Fluid Mech.* **29**, 91–122.

Worster, M. G. 2002 Interfaces on all scales during solidification and melting. In *Interfaces for the Twenty-First Century* (ed. M. K. Smith, M. J. Miksis, G. B. McFadden, G. P. Neitzel & D. R. Canright), pp. 187–201. Imperial College Press.